

produced to afford the thermodynamically more stable O-bonded (alcohol)Cr(CO)₅ products.⁴ Thus, it is possible that there might be statistical influences upon entropies of activation of the numbers of C-H functional groups in the alk molecules employed; these effects, however, are likely to be balanced by similar effects in the hex trap. The nondissociative nature of the rearrangements observed by Xie and Simon⁴ does, however, suggest differing energetically accessible modes of agostic bonding of alk to the metal atom may exist along the reaction coordinate to bond dissociation.

Relationships between the enthalpies of activation for W-alkane bond breaking and W-alkane bond strengths are not yet clearly understood. The observations of Lee and Harris,³ of Hopkins et al.,⁵ and of Joly and Nelson⁶ indicate that vibrational deexcitation accompanies solvent addition to photogenerated [M(CO)₅]. Thus, rates of addition of solvent to thermally equilibrated [M(CO)₅] are not known, although it would seem reasonable to conclude that they are likely to be faster than are those observed for solvent addition to vibrationally excited [M(CO)₅]. This is particularly true, since Hackett, Rayner, and co-workers have shown that the reaction probability for interaction of CH with thermally equilibrated [W(CO)₅] in the gas phase, that is, the ratio of the observed bimolecular rate constant for combination of CH with [W(CO)₅] and the collision diameter, Z_{collis} , is 0.07.²⁰ Thus, the rate of CH addition to [W(CO)₅] is only slightly greater than 1 order of magnitude slower than the gas kinetics reaction cross section. Therefore, on the basis of Hammond's postulate, the activation enthalpy for W-alk bond dissociation to afford thermally equilibrated [W(CO)₅] should closely approximate the bond dissociation energy.

Morse, Parker, and Burkey²¹ have attributed the observed difference between the enthalpy for W-CO bond dissociation in the gas phase, ΔH^\ddagger , 46.0 (28) kcal/mol,²² and the enthalpy of activation for W-CO bond dissociation in alk solution (alk = decalin), 39.9 (16) kcal/mol,²³ to transition-state stabilization due to agostic bonding of alk to W in the latter; in view of the entropies of activation observed here, this would seem not to be an unreasonable conclusion. Taking this difference, 6.1 (44) kcal/mol, into consideration, alk-W bond strengths based on the results obtained here are 14.5 (49) (hep) and 14.3 (48) kcal/mol (CH), in good agreement with the W-hep bond dissociation energy obtained by Burkey et al.²¹ from time-resolved photoacoustic calorimetric data, 13.4 (28) kcal/mol. However, the activation enthalpies reported here (8.4 (5) and 8.2 (4) kcal/mol for alk = hep and CH, respectively) also corresponded closely with W-alkane bond dissociation energies estimated from the equilibrium constants for reversible agostic binding of alkanes to W in (η^1 -alkane)W(CO)₅ complexes, which range from 7.2 (20) to 11.6 (30) kcal/mol;^{20,22} that for (CH)W(CO)₅ is 11.6 (30) kcal/mol.²⁰ It thus will be important to obtain other comparisons of activation enthalpies for solvent dissociation and bond strengths obtained from photoacoustic calorimetric data, as well as more accurate values for bond strengths and activation parameters for CO dissociation from the hexacarbonyls both in the gas phase and in solution, to resolve the substantial uncertainties yet present in the available data.

Acknowledgment. The support of this research by the Robert A. Welch Foundation (Grant B-0434) and the National Science Foundation (Grant CHE-880127) is gratefully acknowledged. Experiments and analyses of the data produced were performed at the Center for Fast Kinetics Research (CFKR) at The University of Texas at Austin. The CFKR is supported jointly by the Biomedical Research Technology Program of the Division of Research Resources of the NIH (Grant RR000886) and by The

University of Texas at Austin. The advice and technical assistance of the staff at the CFKR are much appreciated. We also thank a reviewer for very helpful comments.

Registry No. W(CO)₆, 14040-11-0; hex, 592-41-6; *n*-heptane, 142-82-5; cyclohexane, 110-82-7.

Supplementary Material Available: Appendix I, listing rate constants for reactions taking place after flash photolysis of W(CO)₆ in *n*-heptane/1-hexene and cyclohexane/1-hexene solutions (10 pages). Ordering information is given on any current masthead page.

Contribution from the Laboratoires de Chimie (UA CNRS 1194), Département de Recherche Fondamentale, Centre d'Etudes Nucléaires, 38041 Grenoble Cédex, France

Structural and Redox Properties of the Tempo Adducts of Copper(II) Halides

Jean Laugier, Jean-Marc Latour, Andrea Caneschi,[†] and Paul Rey^{*}

Received February 7, 1991

The coordination chemistry of nitroxide radicals has known in the recent past a surge of interest in relation to their use in the design of molecular magnetic materials.¹ Along these lines, most studies were aimed at developing ferro-² or ferrimagnetic³ interactions between the organic radical and metal ions, so as to obtain molecules possessing the highest possible spin.³⁻⁷

Conversely, the potential use in coordination chemistry of the specific redox properties of nitroxides has been mostly overlooked. Nitroxide radicals can be either oxidized or reduced into, respectively, a nitrosonium or a hydroxylamino ion, and both processes are achievable at easily accessible redox potentials.^{8,9} This justifies that, upon binding to a metal ion, charge transfers can take place, and since several mesomeric forms exist, the actual electronic structure of a complex may, in some cases, be difficult to assess. Electron transfers have been noted during complexation of nitroxides to some metal ions,¹⁰⁻¹⁴ but this kind of chemistry has not been investigated in detail, since the resulting species are generally diamagnetic.

On the other hand, the oxidative properties of nitroxides have been investigated by several authors and an interesting versatility in the oxidation of alcohols has been reported.^{13,15-19} Various methods have been used to generate the nitrosonium ion, which is the active oxidant. These include electrochemistry¹⁷ as well as the use of copper(II) salts.¹³ In the latter case, it is believed that the copper(I) complex that is formed is reoxidized by dioxygen, making the overall process catalytic. However, the exact nature of the species involved in the oxidative transformation is not known.

In the course of our investigations of the coordination chemistry of nitroxides, we have structurally characterized CuBr₂(Tempo) (1), the adduct of Tempo with CuBr₂.²⁰ In this article, in addition to the structural characterization of CuCl₂(Tempo) (2), the adduct of Tempo with CuCl₂, we report an investigation of the solution chemistry and oxidative ability of both compounds. From this study it follows that the active species in the oxidation of alcohols is not the free nitrosonium ion but the copper-tempo complex.

Experimental Section

X-ray Data Collection and Structure Determination. Dark brown crystals of 2 were obtained by using the procedure described for CuBr₂(Tempo).²⁰ They melted at 136 °C, as reported previously.²¹ Preliminary Weissenberg photographs revealed the monoclinic system. Systematic absences ($h0l$, $l = 2n$ and $0k0$, $k = 2n$) were only compatible with the $P2_1/c$ space group. A crystal of approximate dimensions 0.20 × 0.20 × 0.20 mm was mounted on an Enraf-Nonius CAD-4 four-circle

(20) (a) Ishikawa, Y.; Brown, C. E.; Hackett, P. A.; Rayner, D. M. *Chem. Phys. Lett.* **1988**, *150*, 506. (b) Brown, C. E.; Ishikawa, Y.; Hackett, P. A.; Rayner, D. A. *J. Am. Chem. Soc.* **1990**, *112*, 2530.

(21) Morse, J.; Parker, G.; Burkey, T. J. *Organometallics* **1989**, *7*, 2471.

(22) Lewis, K. E.; Golden, D. M.; Smith, G. P. *J. Am. Chem. Soc.* **1984**, *106*, 3905.

(23) Graham, J. R.; Angelici, R. J. *Inorg. Chem.* **1967**, *6*, 2082.

[†] Present address: Department of Chemistry, University of Florence, Florence, Italy.

Table I. Crystallographic Data and Experimental Parameters for $\text{CuCl}_2(\text{Tempo})$ (2)

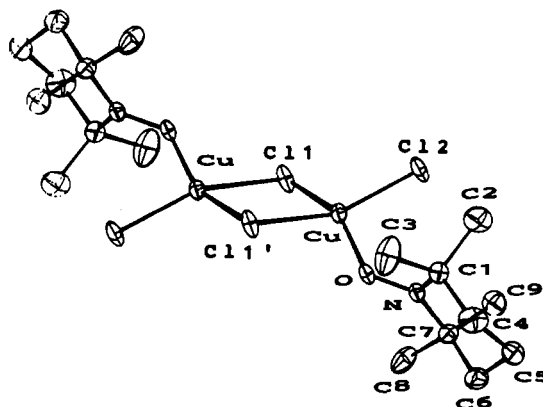
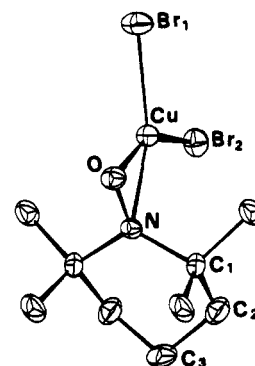
chem formula	$\text{C}_9\text{H}_{18}\text{NOCuCl}_2$	fw	290.7
a , Å	12.045 (5)	space group	$P2_1/c$
b , Å	13.642 (5)	T , °C	20
c , Å	7.679 (3)	ρ_{calc} , g/cm ³	1.55
β , deg	98.46 (2)	μ , cm ⁻¹	9.70
V , Å ³	1248.1	R	0.034
Z	4	R_w	0.036

Table II. Positional Parameters ($\times 10^4$) and B_{eq} Values for $\text{CuCl}_2(\text{Tempo})$ (2)

	x	y	z	B_{eq} , Å ²
Cu	8652 (0)	196 (0)	192 (0)	2.82
Cl1	335 (1)	381 (1)	1941 (1)	4.01
Cl2	2895 (1)	543 (1)	778 (1)	4.52
O	-1884 (1)	1220 (1)	1590 (3)	3.19
N	-2846 (2)	1533 (2)	1836 (3)	2.68
C1	-3262 (2)	1191 (2)	3482 (4)	3.22
C2	-2287 (3)	913 (4)	4812 (5)	7.44
C3	-4010 (3)	299 (3)	3015 (5)	6.13
C4	-3912 (4)	2014 (3)	4217 (5)	5.97
C5	-4675 (3)	2595 (3)	2873 (5)	4.67
C6	-3980 (3)	3034 (3)	1574 (5)	4.41
C7	-3435 (3)	2251 (2)	532 (4)	3.16
C8	-4327 (3)	1724 (3)	-765 (5)	4.68
C9	-2580 (3)	2714 (3)	-481 (5)	5.86

diffractometer equipped with Mo $K\alpha$ radiation and a graphite monochromator. Accurate cell constants were derived from least-squares fitting of the setting angles of 25 reflexions and are reported in Table I with other experimental parameters. The intensities of 2615 reflections ($0 < \theta < 30^\circ$) were collected. Three reflections were periodically checked and showed no significant change during the course of data collection. The data were corrected for Lorentz and polarization factors but not for absorption. Among the independent reflections collected, 2563 had $F_o > 3\sigma(F_o)$ and were used to refine the structural parameters.

The crystal structure was solved by the conventional Patterson method with the SHELX76 package,²² which afforded the positions of the copper

**Figure 1.** Molecular structure of $\text{CuCl}_2(\text{Tempo})$ (2), showing the atom-label scheme. Thermal ellipsoids are drawn at the 30% probability level. Relevant bond lengths (Å) and angles (deg) are as follows: Cu-Cl1 = 2.284 (1), Cu-Cl2 = 2.155 (1), Cu-O = 1.940 (1), O-N = 1.276 (2); Cl1-Cu-Cl'1 = 87.2 (1), Cl1-Cu-Cl2 = 155.0 (1), Cu-O-N = 135.3 (2).**Figure 2.** Molecular structure of $\text{CuBr}_2(\text{Tempo})$ (1), showing the atom-label scheme. Thermal ellipsoids are drawn at the 30% probability level.

- Caneschi, A.; Gatteschi, D.; Sessoli, R.; Rey, P. *Acc. Chem. Res.* **1989**, *22*, 392-398.
- Luneau, D.; Rey, P.; Laugier, J.; Fries, P.; Caneschi, A.; Gatteschi, D.; Sessoli, R. *J. Am. Chem. Soc.* **1991**, *113*, 1245-1251.
- Caneschi, A.; Gatteschi, D.; Laugier, J.; Rey, P.; Sessoli, R.; Zanchini, C. *J. Am. Chem. Soc.* **1988**, *110*, 2795-2799.
- Caneschi, A.; Gatteschi, D.; Laugier, J.; Rey, P. *J. Am. Chem. Soc.* **1987**, *109*, 2191-2192.
- Cabello, C. I.; Caneschi, A.; Carlin, R. L.; Gatteschi, D.; Rey, P.; Sessoli, R. *Inorg. Chem.* **1990**, *29*, 2582-2587.
- Caneschi, A.; Gatteschi, D.; Rey, P.; Sessoli, R. *Inorg. Chem.* **1988**, *27*, 1756-1761.
- (a) Caneschi, A.; Gatteschi, D.; Renard, J.-P.; Rey, P.; Sessoli, R. *Inorg. Chem.* **1989**, *28*, 1976-1980. (b) Caneschi, A.; Gatteschi, D.; Renard, J.-P.; Rey, P.; Sessoli, R. *Inorg. Chem.* **1989**, *28*, 2940-2944.
- Summermann, W.; Deffner, U. *Tetrahedron* **1975**, *31*, 593-596.
- Semmelhack, M. F.; Chou, C. S.; Cortès, D. A. *J. Am. Chem. Soc.* **1983**, *105*, 4492-4494.
- Golubev, V. A.; Voronina, G. N. *Izv. Akad. Nauk. SSSR (Engl. Transl.)* **1972**, *21*, 149-151.
- Takaya, Y.; Matsubayashi, G.; Tanaka, T. *Inorg. Chim. Acta* **1972**, *6*, 339-342.
- Okunaka, M.; Matsubayashi, G.; Tanaka, T. *Bull. Chem. Soc. Jpn.* **1977**, *50*, 907-909.
- Semmelhack, M. F.; Schmid, C. R.; Cortès, D. A.; Chou, C. S. *J. Am. Chem. Soc.* **1984**, *106*, 3374-3376.
- Caneschi, A.; Laugier, J.; Rey, P. *J. Chem. Soc., Perkin Trans.* **1987**, 1077-1079.
- Cella, J. A.; Kelley, J. A.; Keneham, E. F. *J. Org. Chem.* **1975**, *40*, 1860-1862.
- Ganem, B. *J. Org. Chem.* **1975**, *40*, 1998-2000.
- Semmelhack, M. F.; Schmid, C. R. *J. Am. Chem. Soc.* **1983**, *105*, 6732-6734.
- Semmelhack, M. F.; Schmid, C. R.; Cortès, D. A. *Tetrahedron Lett.* **1986**, *27*, 1119-1122.
- Anelli, P.-L.; Biffi, C.; Montanari, F.; Quici, S. *J. Org. Chem.* **1987**, *52*, 2559-2562.
- Caneschi, A.; Grand, A.; Laugier, J.; Rey, P.; Subra, R. *J. Am. Chem. Soc.* **1988**, *110*, 2307-2309.
- Jahr, D.; Rebhan, K. H.; Schwarzhans, K. E.; Wiedemann, J. Z. *Naturforsch.* **1973**, *28B*, 55-62.

ion. Two successive Fourier syntheses allowed the localization of all the remaining non-hydrogen atoms. The structural parameters were refined with anisotropic thermal parameters. In the final refinement model, the hydrogen atoms were included in calculated, fixed positions with isotropic thermal parameters; the final R values are reported in Table I.

Positional parameters are found in Table II. Supplementary material includes a summary of crystal data and experimental X-ray diffraction parameters and listings of bond lengths and angles, anisotropic thermal parameters, and observed and calculated structure factors (Tables SI-SIV); important bond lengths and angles are included in the caption of Figure 1.

Results and Discussion

Solid-State Studies. Complex 2 (Figure 1) is dinuclear, the two $\text{CuCl}_2(\text{Tempo})$ units being doubly bridged by two chloride ions. The two units are related by an inversion center, and as a consequence, the Cu_2Cl_2 fragment is strictly planar. The coordination of the copper atom is best described as D_{2d} -distorted square planar with the Cl(2)-Cu-O plane making a dihedral angle of 34° with the Cu_2Cl_2 plane. The nitrogen atom of the free radical is approximately in the Cl(2)-Cu-O plane, which is roughly perpendicular (97°) to the nitroxide mean plane. There is no pyramidalization of the nitroxide nitrogen as evidenced by the sum of the angles around it, which is 360° within experimental errors. Also of interest is the value of the Cu-O-N angle, which amounts to $135.3(2)^\circ$; this high value as well as the planarity of the Cl(2), Cu, N and O atoms probably results from the minimization of the steric repulsion of the chloride anion with the methyl substituents of the organic ligand. The structural parameters of the nitroxide ligand differ notably from those observed in 1 (Figure 2). Actually, the most important differences reside in the py-

- Sheldrick, G. SHELX76 System of Computing Programs. University of Cambridge, Cambridge, England.

ramidalization of the nitrogen in **1** (28.6°), as compared to about 15° in uncoordinated Tempo²³ and 0° in **2**, and the long N–O distance (1.304 (8) Å in **1** vs 1.276 (2) Å in **2**).

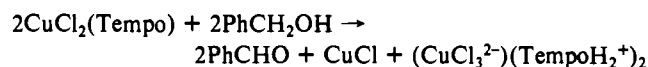
Magnetic susceptibility studies have shown that **1** and **2** are both diamagnetic even at room temperature. In spite of their structural dissimilarity, we think that this diamagnetism has a common origin. **2** can be viewed as a four-spin system. Considering only the exchange couplings between neighbouring spins, one is led to take into account one interaction between the two copper atoms and one within each copper–nitroxide pair. The interaction between the two copper atoms is not likely to give a strong antiferromagnetic coupling: (i) according to magneto-structural correlations in chloro-bridged dimers, the value of the ratio of the bridge angle (Cu–Cl(1)–Cu' = 92.8°) to the copper-bridging chlorine distance (average Cu(1)–Cl(2) = 2.31 Å) corresponds to a weak coupling constant ($|J| < 1 \text{ cm}^{-1}$);²⁴ (ii) the D_{2d} distortion lessens the overlap between the orbitals of the metal ions and those of the bridging atoms, thus reducing the exchange.²⁵ On the other hand, the interaction of a copper ion with an equatorially bound²⁶ nitroxide is known to lead to a very strong antiferromagnetic coupling ($|J| > 500 \text{ cm}^{-1}$).^{1,26,27} Such high values can be easily rationalized by considering that, in those situations where the Cu–O–N angle differs from 180°, the Cu $d_{x^2-y^2}$ and the nitroxide π^* orbitals have a nonzero overlap. Moreover, the closer to 90° this angle, the larger the coupling, as predicted by theoretical calculations²⁸ and experimentally observed.^{1,26} Thus, a value of 135.3° for this angle is quite consistent with the observed diamagnetism of **2**, resulting from the contribution of two diamagnetic copper–nitroxide units.

The electronic structure of **1** has been investigated through ab initio calculations.²⁹ Mulliken population analysis definitely rules out any electron transfer from or to the nitroxide ligand, thus supporting the Cu²⁺(Tempo[•]) formulation over the two other mesomeric forms Cu³⁺(Tempo⁻) and Cu⁺(Tempo⁺). Therefore, the diamagnetism of the complex is well understood if one considers that the structural arrangement with the CuBr₂NO plane perpendicular to the mean plane of the nitroxide is the one most favorable²⁸ to a strong σ overlap of the magnetic orbitals of the two moieties. In addition, both the Cu–O and the Cu–N bond lengths are rather short, which again improves the overlap. Although equatorial bonding of a nitroxide to a copper(II) ion is known to lead to high antiferromagnetic interactions as observed in **2**, the novel side-on binding mode found in **1** is likely to give rise to even more strongly coupled systems. In this respect, it is worth noting that the ab initio calculations estimate at 5000 cm⁻¹ the lower limit of the singlet–triplet gap in this compound.²⁹

Solution Studies. Although the complexes are indefinitely stable in the solid state in dry atmospheres, they decompose slowly in the presence of moisture and very rapidly in the presence of water or alcohols. **1** is stable in dichloromethane and does not dissociate, since an osmometric determination gave a molecular weight of 362 (20), which is close to the theoretical value of 379. Also, conductivity measurements in this solvent reveal that both complexes behave as nonelectrolytes. Moreover, electronic absorption spectra of the two compounds in this solvent show the presence of strong charge-transfer transitions near 300 nm. Therefore, the two compounds retain their integrity in dichloromethane solution.

In order to get a deeper insight into the mechanism of the oxidation of alcohols by these systems, we investigated the reaction of benzyl alcohol with **1** and **2** in dichloromethane. The reaction

of PhCH₂OH with 1 equiv of **1** or **2** at room temperature affords benzaldehyde in quantitative yield. Copper(I) chloride and the trichlorocuprate(I) salt of the protonated hydroxylamine³⁰ (CuCl₃²⁻)(TempoH₂⁺)₂ have been isolated at the end of the reaction, which can thus be written as



Interestingly, the reactions with **1** and **2** proceed at very different rates. In the case of **1**, following the formation of the aldehyde by gas chromatography, the reaction was found first order in each of the reactants. On the other hand, with **2**, the reaction was so fast that no kinetic information could be obtained by standard techniques. Preliminary experiments have shown that this reduced reactivity of the bromo derivative gives rise to a selective system. Actually, while primary alcohols like 1-octanol are oxidized by **1** at ambient temperatures in the aldehyde (1-octanal), secondary alcohols (3-octanol, for example) are not; however, they can still be oxidized at 50 °C in the corresponding ketone (3-octanone).

In the recent past, Semmelhack has presented a thorough mechanistic study of alcohol oxidation by Tempo[•] in solution.¹⁸ Among the various possible pathways, the formation of a reactive adduct by nucleophilic addition to the nitrogen atom of the nitroxide followed by proton abstraction by internal and external bases was the preferred route. Nevertheless, this mechanism does not account for the different reactivities that we observed for **1** and **2** in dichloromethane. As shown by ab initio calculations, the complexation of Tempo by the copper salt does not involve an electron transfer between the two fragments. In pure dichloromethane, the integrity of the copper–nitroxide complex is retained as evidenced by the osmometric and conductometric measurements. The reaction of either **1** or **2** with various potential ligands provides interesting additional information. Actually, when a dichloromethane solution of one of these complexes is treated by pyridine, Tempo⁰ is liberated. On the other hand, no reaction is observed at room temperature in the presence of the nonoxidizable 2-propanol, which means that weak ligands like alcohols are not able to displace the coordinated nitroxide. From the whole set of experimental findings the following mechanistic implications can be drawn: (i) the active catalyst is not the free nitrosonium ion but the nitroxide complex; (ii) the alcohol does not enter the first coordination sphere of the copper ion. This proposition does not strictly exclude the formation of the binary adduct proposed by Semmelhack, but rules out that, in this case, it be formed from the nitrosonium ion. Therefore, it is likely that the reaction involves the initial formation of a ternary adduct [CuX₂–Tempo–alcohol]. Electron and proton transfers could occur within the ternary adduct, or alternatively, the addition of the alcohol to the coordinated nitroxide would induce the electron transfer and the liberation of the intermediate postulated by Semmelhack. According to this scheme, the difference in the reactivities of **1** and **2** must have its origin either in the different electronic structures of the complexes or in different accessibilities of the bound nitroxide for the substrate. Investigation of the steric aspects of the problem with the help of molecular graphics software definitely rules out that steric hindrance plays a major role. However, the observed difference in reactivity parallels that noted in the NO bond lengths. Although no net electron transfer on the nitroxide is occurring, the longer NO bond in **1** points to subtle electronic redistribution in the complex. This suggests that, upon formation of the ternary adduct, electron transfer depends on the intimate electronic structure of the complex. So the nature of the copper counteranion effectively tunes the oxidative ability of the system rendering it very selective in the oxidation of alcohols.

Acknowledgment. We thank the Region Rhone-Alpes for financial support in the framework of the Programme Chimie Fine and Dr. P. Maldivi for assistance in the use of the molecular

- (23) Capiomont, A.; Lajzerowicz-Bonneteau, J. *Acta Crystallogr.* **1974**, *B30*, 2160–2166.
 (24) Willett, R. W. *Magneto-Structural Correlations in Exchange Coupled Systems*; Willett, R. D., Gatteschi, D., Kahn, O., Eds.; NATO ASI Series C140; Kluwer: Boston, MA, 1985; pp 389–420.
 (25) Chiari, B.; Piovesana, O.; Tarantelli, T.; Zanazzi, P. F. *Inorg. Chem.* **1987**, *26*, 952–955.
 (26) Dickman, M. H.; Doedens, R. J. *Inorg. Chem.* **1981**, *20*, 2677–2681.
 (27) Lim, Y. Y.; Drago, R. S. *Inorg. Chem.* **1972**, *11*, 1334–1338.
 (28) Caneschi, A.; Gatteschi, D.; Grand, A.; Laugier, J.; Pardi, L.; Rey, P. *Inorg. Chem.* **1988**, *27*, 1031–1035.
 (29) Rohmer, M.-M.; Grand, A.; Benard, M. J. *Am. Chem. Soc.* **1990**, *112*, 2875–2881.

- (30) Characterization of this compound was based on the following observations: (i) the elemental analysis corresponds to the proposed formula; (ii) treatment with dilute aqueous sodium hydroxide affords the hydroxylamine.

graphics software (Sybyl). A.C. gratefully acknowledges financial support from the Commissariat à l'Energie Atomique during a 1-year stay in Grenoble, France.

Registry No. 1, 113132-33-5; 2, 136246-87-2; PhCH₂OH, 100-51-6; PhCHO, 100-52-7.

Supplementary Material Available: Listings of crystal data and experimental parameters (Table SI), bond lengths and angles (Table SII), and anisotropic thermal parameters (Table SIII) (3 pages); a listing of observed and calculated structure factors (Table SIV) (13 pages). Ordering information is given on any current masthead page.

Contribution from the Department of Inorganic Chemistry, H. C. Ørsted Institute, University of Copenhagen, Universitetsparken 5, DK-2100 Copenhagen, Denmark, and Haldor Topsøe Research Laboratories, Nymøllevej 55, DK-2800 Lyngby, Denmark

ESR Spectra of Hexaaquamolybdenum(III) Ions in Cesium Indium Alum

Claus J. H. Jacobsen^{1,2} and Erik Pedersen^{*2}

Received June 5, 1991

The isolation and characterization of transition-metal aqua ions is an area of considerable interest. Hexaaquachromium(III) ions are well characterized³ and have been known for a long time, but it was not until 1986 that a convenient route to the congeneric hexaaquamolybdenum(III) ions was published⁴ and still hexaaquatungsten(III) ions are unknown. When the coordination chemistry of chromium(III) and molybdenum(III) is compared, it is immediately conspicuous that only relatively few classical Werner-type molybdenum(III) complexes are known. Consistent with this, several reports concerning the ESR spectrum of hexaaquachromium(III) ions diluted in diamagnetic alums have appeared.⁵ In 1977, the ESR spectrum of hexaaquamolybdenum(III) ions diluted in ammonium aluminum alum was reported.⁶ Unfortunately, this report seems to be erroneous, and we decided, therefore, to undertake this study.

Experimental Section

Synthesis. All operations were carried out under dinitrogen using Schlenk equipment and standard vacuum techniques. The chemicals used were of analytical grade and were used without further purification.

Hexaaquamolybdenum(III) ions obtained directly from cesium molybdenum alum as well as from hydrolyzed sodium hexakis(formato)molybdate(III) were diluted in cesium indium alum by the following procedure: 16.8 mg of sodium hexakis(formato)molybdate(III) or 24.2 mg of cesium molybdenum alum⁴ (38.6 μmol) was added with stirring to a solution of 1.00 g (1.93 mmol) of In₂(SO₄)₃ in 10 mL of 1 M sulfuric acid. Immediately thereupon 0.70 g (1.93 mmol) of Cs₂SO₄ was added, and within a few seconds the molybdenum(III)-doped cesium indium alum precipitated. This was washed twice with 10 mL of 96% ethanol and dried in vacuum. Molybdenum-doped ammonium aluminum alum was prepared by an analogous procedure. The molybdenum content was not analyzed but assumed to be approximately 1%.

ESR Spectra. X-band spectra of powdered samples at 6 and 70 K were recorded with a Bruker ESP 300 spectrometer equipped with an Oxford ESR-900 continuous-flow cryostat and operating at 9.37 GHz. All spectra were obtained by averaging 10 scans using a modulation

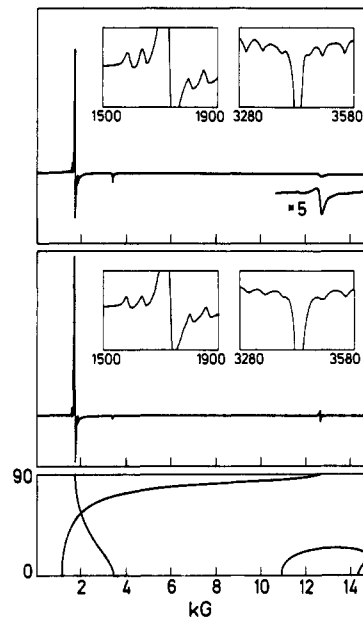


Figure 1. Top: Powder ESR spectrum of 1% hexaaquamolybdenum(III) ions diluted in cesium indium alum measured at 6 K. Detailed spectra showing the hyperfine structure of both the *xy* transition at approximately 1740 G and the *z* transition at 3425 G are included. The signal appearing as a shoulder at 3463 G in the spectrum of the *z* transition is due to an unidentified impurity. Middle: Result of simulating the ESR spectra with the spin-Hamiltonian parameters given in Table I and line widths of 10 G. Bottom: Angular dependence of the line positions as a function of the angle between the molecular *z* axis and the magnetic field. For clarity the isotopes with nonzero nuclear spin have been excluded.

Table I

g_{\parallel}	g_{\perp}	$ D /\text{cm}^{-1}$	$10^4 A_{\parallel} /\text{cm}^{-1}$	$10^4 A_{\perp} /\text{cm}^{-1}$
1.954	1.950	1.15	50.5	47.3

frequency of 100 kHz with an amplitude of 2.88 G. The magnetic field range was 50–15 050 G.

Results and Discussion

The ESR spectrum of hexaaquamolybdenum(III) ions diluted in cesium indium alum measured at 6 K is shown in Figure 1 together with the computer-simulated spectrum and a diagram showing the angular dependence of the line positions. We chose the cesium indium alum as a diamagnetic matrix since this is known to be a β -alum⁷ just as the cesium molybdenum alum.⁸ Furthermore, the ionic radii of the hexaqua complexes of indium(III) and molybdenum(III) are expected to be similar. In an alum the site symmetry of the hexaaquamolybdenum(III) ions is S_6 , i.e. a trigonally distorted environment. In accordance with this the spectrum can be interpreted in terms of the conventional spin Hamiltonian for a d^3 ion in axial symmetry, i.e. a quartet ground state:

$$\hat{H} = \mu_B \mathbf{H} \cdot \mathbf{g} \cdot \hat{\mathbf{S}} + \hat{\mathbf{S}} \cdot \mathbf{A} \cdot \hat{\mathbf{I}} + D(\hat{S}_z^2 - \frac{1}{3}S(S+1)) = \mu_B(g_{\parallel}H_z\hat{S}_z + g_{\perp}(H_x\hat{S}_x + H_y\hat{S}_y)) + A_{\parallel}\hat{S}_z\hat{I}_z + A_{\perp}(\hat{S}_x\hat{I}_x + \hat{S}_y\hat{I}_y) + D(\hat{S}_z^2 - \frac{1}{3}S(S+1)) \quad (1)$$

Naturally occurring molybdenum consists of several isotopes of which ⁹⁵Mo (15.72%) and ⁹⁷Mo (9.46%) are the only ones having a nonzero nuclear spin ($I_{\text{Mo}} = 5/2$). These two nuclides have slightly different magnetic moments, but the difference is too small to be observed in our ESR data. This means that an ESR spectrum of monomeric molybdenum(III) in ideal cases will consist of one or more groups of lines, each group having one relatively strong center line and six hyperfine lines, the intensities

(1) University of Copenhagen.
 (2) Haldor Topsøe Research Laboratories.
 (3) Bjerrum, N. Z. *Phys. Chem.* **1907**, *59*, 336. Hunt, J. P.; Taube, H. J. *Chem. Phys.* **1950**, *18*, 757.
 (4) Brorson, M.; Schäffer, C. *Acta Chem. Scand., Ser. A* **1986**, *A40*, 358.
 (5) E.g.: Bagguley, M. S.; Griffiths, J. H. E. *Proc. R. Soc. A* **1950**, *204*, 203. Danilov, A. G.; Manoogian, A. *Phys. Rev. B* **1972**, *6*, 4097.
 (6) Radhakrishna, S.; Chowdari, B. V. R.; Kasi Viswanath, A. *J. Chem. Phys.* **1977**, *66*, 2009.

(7) Beattie, J. K.; Best, S. P.; Skelton, B. W.; White, A. H. *J. Chem. Soc., Dalton Trans.* **1981**, 2105.

(8) Brorson, M.; Gajhede, M. *Inorg. Chem.* **1987**, *26*, 2107.